Computer simulation of hydrogen diffusion and nuclear magnetic relaxation on a disordered lattice

1995 J. Phys.: Condens. Matter 7 7501

(http://iopscience.iop.org/0953-8984/7/38/009)

J. Phys.: Condens. Matter 7 (1995) 7501–7516. Printed in the UK

Computer simulation of hydrogen diffusion and nuclear magnetic relaxation on a disordered lattice

Lu Hua, J M Titman and R L Havill
Department of Physics, The University of Sheffield, Hounsfield Road, Sheffield S3 7RH, UK

Received 3 July 1995

Abstract. The dipolar nuclear magnetic relaxation rate associated with the hopping diffusion of interstitial hydrogen atoms in a disordered alloy is calculated by Monte Carlo methods. The principal features of the model system are that the atoms hop on a spatially disordered array of traps and the trapping energy varies from trap to trap so that the diffusion of the hydrogen is characterized by a distribution of jump rates. The effective jump rate from a trap is assumed to have an Arrhenius dependence on temperature causing the distribution of jump rates to depend on temperature. Unlike earlier work, the method fully explores the way in which this dependence affects the mean jump rate as well as providing the means to calculate the relaxation as a function of both Larmor frequency and temperature. The mean jump rate is found to deviate from the Arrhenius form in a manner that depends on the concentration of the hydrogen nuclear spins. At a given temperature the characteristic peak in the relaxation rate, which occurs in ordered solids when the product of the average jump rate and the Larmor frequency is approximately unity, is broadened, becomes asymmetric and is shifted in frequency by the presence of the jump rate distribution. The broadening is found to be less apparent when the relaxation rate is calculated as a function of temperature but the asymmetry remains.

1. Introduction

In metals and alloys containing absorbed hydrogen, the hydrogen atoms occupy interstitial sites in the metal lattice and, except at very low temperatures where there may be tunnelling effects [1], diffuse among these sites by a hopping mechanism. In amorphous alloys the individual sites may have different structural and chemical environments resulting in a range of binding and activation energies which give rise to a distribution of hopping rates. Nuclear magnetic relaxation due to the interaction of the nuclear spin dipoles on the hydrogen atoms is often used to measure diffusion rates. In ordered alloys theoretical models based on lattice diffusion [2, 3] are used to calculate the longitudinal dipolar relaxation rate, T_1^{-1}, and allow the hopping rate of the hydrogen to be extracted from the experimental data. Such models are capable of giving analytical results for ordered materials but, because of the relative complexity of the problem, the construction of theoretical models for disordered alloys is a more difficult task. Some recent work by Sholl, however, points the way to a theoretical solution by numerical methods [4]. The Monte Carlo (MC) method, which is complementary to the theoretical approach, has many advantages for relaxation in amorphous alloys, principally because dealing with disorder is a daunting theoretical task whereas in MC simulation the inclusion of a wide range of different types of disorder is straightforward.

Theoretical models for ordered materials are aimed at the calculation of the relaxation rate as a function of the average interval between hops of the spin dipoles, $\bar{\tau}$. On the

0953-8984/95/387501+16$19.50

other hand, the most obvious experimental methods measure its variation with temperature and the contact between theory and experiment is made by assuming an Arrhenius relation between $\bar{\tau}$ and the temperature. Such a simple assumption can not be made for disordered systems if the distribution of jump rates is also temperature dependent. Such a temperature dependence occurs in activated processes even if the energy distribution itself is temperature independent and in such cases $\bar{\tau}$ does not necessarily follow the Arrhenius law as we will show for a chosen example of disorder. In previous work using MC simulation the dipolar relaxation rate in disordered systems [5, 6, 7] has been calculated in terms of frequency at a given temperature mainly because the most straightforward calculations involve the time dependence of the spin dipolar correlation function. The temperature dependence of the relaxation rate has been largely ignored.

Nevertheless, some efforts have been made to calculate the temperature dependence of the relaxation rate [7, 8]. In particular, one example involving two of the present authors [7] attempted to obtain the temperature dependence by comparison with the long-range diffusion. Temperature was not explicitly part of the model and use of long-range diffusion in this way is open to question since the relaxation is related to the motion of the spins over relatively short times, that is, comparable with $\bar{\tau}$. The purpose of the present work is to develop a computer model in which temperature is an explicit parameter and to use it to calculate the temperature dependence of the dipolar relaxation time, T_1. Since computer simulation methods inevitably follow the time evolution of the atomic positions, the calculation of the relaxation rate at a given temperature involves two steps, one finding the spin correlation function in terms of $\bar{\tau}$ and the other essentially determining the value of $\bar{\tau}$ at that temperature. It is, of course, possible to present the results simply as graphs of T_1 against temperature. However, we have found that there are interesting aspects of $\bar{\tau}$ which are worth reporting and we present our method as first involving the calculation of the temperature dependence of the average interval between hops of the spins, $\bar{\tau}$, before finding the spin correlation function in terms of $\bar{\tau}$ from the same MC procedure. The relaxation time as a function of temperature is obtained by combining the results of these simulations. We are able to show that the disorder causes $\bar{\tau}$ to depart from the usual Arrhenius behaviour and the effective activation energy over a limited range of temperature changes in a characteristic manner with composition. The MC calculations establish the relation between the relaxation rate and temperature, which, in principle, allows experimental measurements of the relaxation to be exploited to find $\bar{\tau}$ in the presence of energy disorder.

2. The model

Many aspects of the present computer model are the same as those of Adnani *et al* [7]. In disordered alloys the hydrogen atoms, which carry a nuclear spin $I = \frac{1}{2}$, diffuse by hopping on a network of interstitial sites in the metal matrix. The nuclear magnetic relaxation arises from the random fluctuations of the magnetic dipole coupling between the spins caused by the motion. For the MC simulation the network of interstitial sites is modelled by a simple cubic lattice which has been distorted to approximate the structural disorder of an amorphous alloy. The hydrogen atoms have to overcome an energy barrier to jump to a neighbouring site. This energy can be divided into two parts, the site energy, which is the energy required to escape the bonding force at the site, and the saddle point energy, which is the barrier between neighbouring sites. The metal atoms surrounding the interstitial sites are not all identical in an alloy and this, coupled with the structural disorder, is assumed to cause a random variation from site to site in both these energies. There is some evidence that disorder in the site energy has more effect on the relaxation rate, particularly at low

concentration [6]. The assumption is in this work that there is no spread in the saddle point energy and it is conveniently set to zero so that the spin need only overcome the site binding energy to hop to a neighbouring site if it is not occupied. For simplicity the site energy distribution is assumed to be uniform in the range

$$\hat{E} - \delta E/2 < E < \hat{E} + \delta E/2 \tag{1}$$

where $\hat{E}$ is the mean and δE is the width. Because the saddle point energy is zero this distribution alone reflects the distribution in the activation energy of the hopping process.

In addition to the energy barriers the fraction of the available sites occupied by the spins affects the diffusion. The greater the concentration the fewer free sites there are to accommodate hops and the more likely it is for a spin to make return hops to the previously occupied site. The model simulates different concentrations by changing the number of spins in the system and the computer program was written in such a way that this does not affect the efficiency very much. The principal difference between the present work and that of Adnani *et al* [7], in addition to the main point of the work which is to introduce the temperature dependence, lies in the method used to simulate the hopping mechanism of the spins.

3. The average hopping rate

Before dealing with the diffusion by the MC model we will draw a number of conclusions regarding the average hopping rate which will serve to describe the boundaries of the problem. We assume that at finite temperatures a spin can jump out of the energy well on the site where it resides at the rate, ν. This hopping rate is related to the site energy through the Arrhenius rule,

$$\nu = \nu_0 e^{-E/kT} \tag{2}$$

where ν_0 is the attempt frequency of the classic diffusion model and k is the Boltzmann constant. In this work ν_0 is assumed to be a constant, independent of temperature. This may not be entirely true in real materials but it is assumed to be a reasonable approximation since there is no evidence as far as we know that suggests a strong variation with temperature. Due to the spread in site energy equation (2) leads to a distribution of hopping rates. At temperature T the highest and lowest rates which correspond to the extremes of the site energy are

$$\nu_{max} = \nu_0 e^{-(\hat{E}-\delta E/2)/kT} \qquad \nu_{min} = \nu_0 e^{-(\hat{E}+\delta E/2)/kT}. \tag{3}$$

The hopping rate distribution function, derived from the uniform distribution of site energy, is

$$\rho(\nu) = kT/\nu\,\delta E = 1/n\hat{\nu}\ln(r) \qquad \text{with } r = \nu_{max}/\nu_{min} = e^{\delta E/kT} \text{ and } \nu = n\hat{\nu} \tag{4a}$$

where $\hat{\nu} = \nu_0 \exp(-\hat{E}/kT)$ is the hopping rate associated with the mean energy and $\rho(\nu)$ is normalized to unity in the interval $r^{-1/2} < n < r^{1/2}$. We have written $\rho(\nu)$ in this form to show that, apart from the multiplier, $\hat{\nu}$, it is completely specified by the choosing r, the ratio between the limiting values of ν. As will become apparent below, the absolute value of $\hat{\nu}$ is not required in the calculation of the spin correlation functions.

In the present work, in which the temperature dependence of the ratio, r, is to be displayed explicitly, it is convenient to assume that at a certain temperature T_0 the value of this ratio is r_0, so that we can use T_0 and r_0 as two basic parameters of the model. In the

following temperature and energy are given in units of T_0 and kT_0, that is $T = \Theta T_0$ and $E = \mathcal{E}kT_0$, respectively. The hopping rate distribution function then becomes

$$\rho(\nu) = \Theta/n\hat{\nu}\ln(r_0) \qquad r = e^{\delta\mathcal{E}/\Theta} \tag{4b}$$

where $\rho(\nu)$ is normalized to unity in the interval

$$r_0^{-1/2\Theta} < n < r_0^{1/2\Theta}.$$

The increase of r as the temperature decreases and the change in the distribution $\rho(\nu)$, are then immediately apparent from these equations.

The distribution function $\rho(\nu)$ in equation (4) reflects only the property of the sites on which the hydrogen atoms or spins diffuse. The rate distribution function of the spins themselves $\rho_s(\nu)$ may be influenced by other factors such as temperature and the fractional occupancy, c, of the available sites by the spins. In order to derive $\rho_s(\nu)$ when the system is in equilibrium and, in turn, determine the average hopping rate, $\bar{\nu}$, we need to know how the spins are distributed among the various sites.

We first discuss two extreme cases. In the first place, if the concentration is very high and most of the available sites are occupied, $\rho_s = \rho$ to a good approximation. Secondly, if the concentration is low the spins will tend to occupy sites with greater binding energy and we may suppose that the spin distribution is skewed by a Boltzmann factor. The presence of this factor means that the probability of a spin occupying a site with site energy E is proportional to $e^{E/kT}$, which, according to equation (2), is in turn proportional to $1/\nu$. By combining this Boltzmann factor with $\rho(\nu)$ we have

$$\rho_s(\nu) = \frac{\nu_{max}\nu_{min}}{\nu_{max} - \nu_{min}}\frac{1}{\nu^2} = \frac{\nu_0 \exp\left(-\hat{\mathcal{E}}/T\right)}{r_0^{1/(2\Theta)} - r_0^{-1/(2\Theta)}}\frac{1}{\nu^2} \tag{5}$$

normalized to unity in the interval $\nu_0\exp(-\hat{\mathcal{E}}/\Theta)r_0^{-1/(2\Theta)} < \nu < \nu_0\exp(-\hat{\mathcal{E}}/\Theta)r_0^{1/(2\Theta)}$.

The average hopping rates, $\bar{\nu}$, under these extreme conditions can be calculated from the two distribution functions for very high and very low spin concentrations. For the high concentration we use equation (4) to give

$$\bar{\nu}_H = \int_{\nu_{min}}^{\nu_{max}} \rho(\nu)\nu\ \mathrm{d}\nu = \frac{\Theta}{\ln(r_0)}(\nu_{max} - \nu_{min}) = \frac{\nu_0\Theta}{\ln(r_0)}\left(r_0^{1/(2\Theta)} - r_0^{-1(2\Theta)}\right)e^{-\hat{\mathcal{E}}/\Theta} \tag{6}$$

that is

$$\bar{\nu}_H = \nu_0 f(\Theta, r_0)\exp(-\hat{\mathcal{E}}/\Theta) = f(\Theta, r_0)\hat{\nu} \tag{7}$$

where

$$f(\Theta, r_0) = \Theta(r_0^{1/(2\Theta)} - r_0^{-1/(2\Theta)})/\ln(r_0). \tag{8}$$

At the low concentration ρ_s of equation (5) is the more appropriate form giving

$$\bar{\nu}_L = \int_{\nu_{min}}^{\nu_{max}} \rho_s(\nu)\nu\ \mathrm{d}\nu = \frac{\nu_0\ln(r_0)}{\Theta}\frac{e^{-\hat{\mathcal{E}}/\Theta}}{\left(r_0^{1/(2\Theta)} - r_0^{-1/(2\Theta)}\right)} \tag{9}$$

that is

$$\bar{\nu}_L = \nu_0 f(\Theta, r_0)^{-1}\exp(-\hat{\mathcal{E}}/\Theta) = f(\Theta, r_0)^{-1}\hat{\nu}. \tag{10}$$

When there is no spread of site energy equations (7) and (10) both reduce to the standard Arrhenius form for hopping diffusion. Also it can be shown straightforwardly that, given r_0 is finite, $f(\Theta, r_0) \to 1$ when $\Theta \to \infty$. From this we conclude that when there is a spread in site energy the mean hopping rate deviates from the Arrhenius rule. The extent of

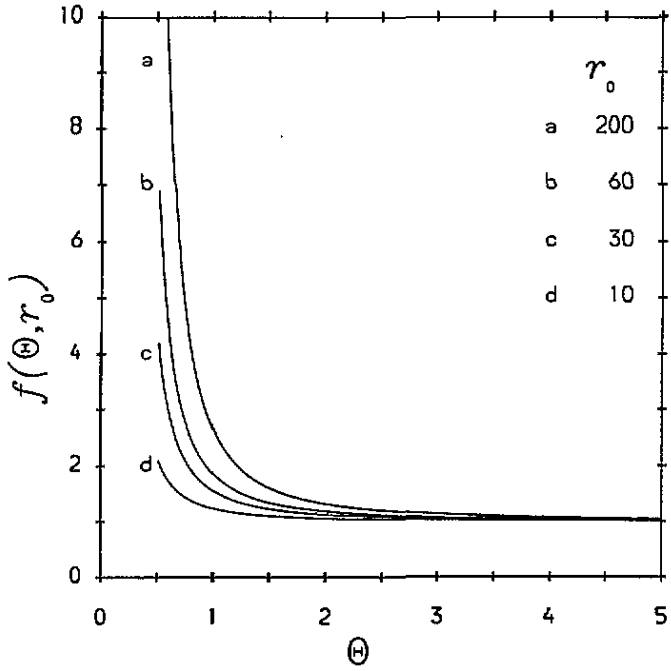

Figure 1. As explained in the text the spread of site energies, which depends on the reduced temperature Θ and is defined by the parameter r_0, causes the mean hopping rate to deviate from the Arrhenius law. The extent of the deviation is governed by the factor $f(\Theta, r_0)$, which is shown in the figure as a function of Θ for several values of r_0.

the deviation is determined by the function $f(\Theta, r_0)$ which is shown in figure 1 for several values of r_0.

In the above $\bar{\nu}_H$ and $\bar{\nu}_L$ are strictly the averages over the equilibrium distribution functions and whether they truly represent the average jump rates needs to be tested by the MC simulation. In the present model at low concentration the motion of each spin is independent of the others and each jump is independent of the previous one because the binding energies are distributed in a random way over the matrix of sites and each energy is attached to an individual site. Under these circumstances the effect of a finite concentration can be limited to a factor, $1 - c$ where c is the spin concentration, multiplying the hopping rate in equation (10). This factor takes into account the reduced availability of vacant neighbouring sites into which spins can jump. At high concentration the probability of a jump depends on the immediate neighbours around each vacancy and it is not clear that the simple average $\bar{\nu}_H$ is applicable in this case. The factor of $1 - c$ still applies however, together with any effects from the more highly correlated motion.

The form of equations (7) and (10) also suggests an interpolation, linear in c, which could be applied to find the average jump rate for an arbitrary spin concentration. That is, we write

$$\bar{\nu}/\nu_0 = f(\Theta, r_0)^{2c-1} e^{-\hat{\varepsilon}/\Theta} \tag{11}$$

$$\bar{\tau}/\tau_0 = f(\Theta, r_0)^{1-2c} e^{\hat{\varepsilon}/\Theta}. \tag{12}$$

We have introduced the mean interval between hops, $\bar{\tau} = 1/\bar{\nu}$, and $\tau_0 = 1/\nu_0$ in equation (12) because nuclear magnetic relaxation rates are usually expressed in terms of $\omega\bar{\tau}$, where

ω is the Larmor frequency. This interpolation is highly speculative but along with the expressions for $\bar{\nu}_H$ and $\bar{\nu}_L$ it provides a framework for the calculation of the mean hopping rate by the MC method. In what follows we will show that our MC simulation demonstrates the validity of these equations.

4. The Monte Carlo simulation of the diffusion

In the MC simulation N_s spins diffuse on a distorted cubic lattice under periodic boundary conditions which are there to remove surface effects and prevent the loss of spins. Each lattice point has six nearest neighbours and is assigned a site energy from the distribution defined in equation (1) so that the resultant distribution in hopping rates is $\rho(\nu)$ given in equation (4). The pre-exponential factor is a constant and can be used as the unit of the hopping rate. During one MC step each of the spins makes an attempt to jump to its neighbouring site. At each attempt an MC procedure is carried out to test whether an attempt is successful. The procedure consists of two stages, the first being an attempt by the spin to escape from the site and the second being the possibility of moving into a vacant site. To carry out this procedure a number n_i between zero and unity is chosen at random and compared with the hopping rate ν_i associated with the site on which the spin i resides. If $n_i < \nu_i$ the first stage of the jump is successful. One direction from the six is chosen at random and, if the neighbouring site in that direction is vacant, the jump is made and the event is successful.

During each MC step only a fraction of the total number of attempts is successful and accepted. The acceptance rate, p, which we define as the number of accepted events divided by the total number of spins in the system, depends on the spin concentration, the temperature and the energy distribution. For example, at a given energy distribution p decreases as the temperature is lowered and the efficiency of the MC calculation diminishes. In order to keep the acceptance rate at a suitable value on average under all conditions, the actual hopping rates were multiplied by a factor Δ, which was adjusted according to the requirements of the simulation.

On average all the spins jump in a period equal to mean time between jumps, $\bar{\tau}$ [7]. Thus τ can be defined as the mean period in which N_s successful jumps take place and in computer units this is the number of MC steps required for these N_s jumps. Given the above definition of p the mean interval, $\bar{\tau}$, satisfies the relation $\bar{p}\bar{\tau} = 1$, where $\bar{p}$ is the average acceptance rate per step. In this equation Δ has been assumed to be unity. If the value of Δ is changed, $\bar{p}$ changes proportionately so that $\bar{p}\bar{\tau} \propto \Delta$. This relation leads directly to the useful equation

$$\bar{p}\bar{\tau}/\bar{p}_0\bar{\tau} = \Delta/\Delta_0 \qquad \text{or} \qquad \bar{\tau} = \bar{\tau}_0\ \bar{p}_0\Delta/\bar{p}\Delta_0 \tag{13}$$

in which the subscript 0 indicates that the quantities are determined at a reference temperature. From this equation values of the mean interval between jumps at different temperatures may be calculated relative to one another. The factor, Δ, is not a function of temperature but is changed only to keep the acceptance rate at a reasonable level in order that the efficiency is not seriously affected and there are a reasonable number of MC steps in the interval $\bar{\tau}$. Without attention to the latter there could be too few data points in the spin correlation functions. The adjustments to Δ were made under the restriction that the highest hopping rate was less than unity, the maximum value given by the random number generator.

The spin densities and $\bar{\tau}$ were calculated from the MC simulation after an initial stage to obtain thermal equilibrium. Figure 2 shows how the jump rate distribution function depends

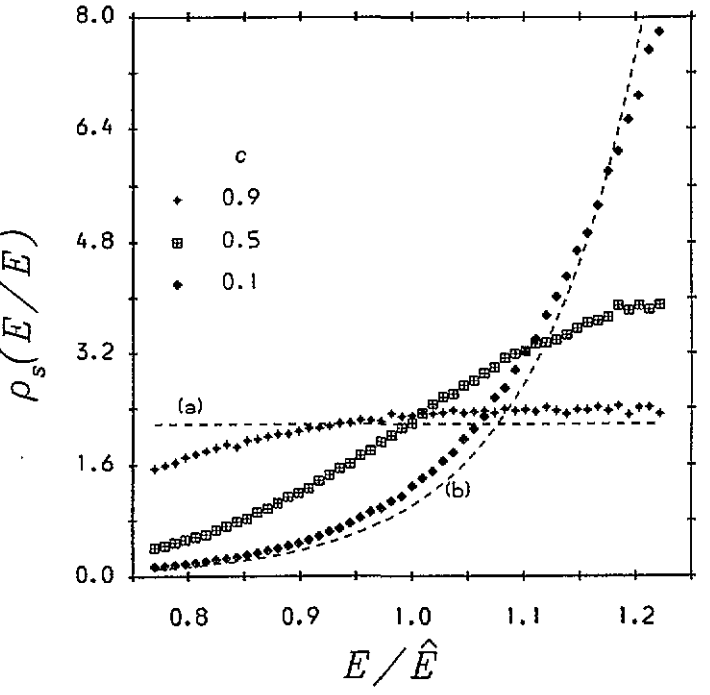

Figure 2. Simple arguments lead to the conclusion that energy distribution, ρ_s, of the hydrogen atoms is equal to the distribution, ρ, of site energies, E, when the concentration, c, approaches unity. The condition, $\rho_s = \rho$ as a function of energy is given by the horizontal line (a). On the other hand at low concentration ρ_s is modified by a Boltzmann term which, as shown by curve (b), increases the population of the sites for which E is large and negative. The data points show the extent to which these ideal conditions are satisfied in the MC simulation.

on the spin concentration. In this figure the distribution, $\rho_s(E/\hat{E})$, is given in terms of the energy rather than ν so that the horizontal line (a) represents the condition $\rho_s = \rho$ and the line (b) is the form of $\rho_s(E/\hat{E})$ at $c \to 0$. The coincidence between the MC calculation and the analytical forms at these extremes is clearly seen. These results give us confidence that the simulation can correctly predict the equilibrium conditions.

The data points of figure 3 show the results of the MC calculations of $\bar{\tau}/\tau_0$, displayed as a function of temperature. The dashed lines are the values of $\bar{\tau}/\tau_0$ at $c = 0$ and 1 and the solid lines are obtained from the interpolation of equation (12). The general agreement between the simulation and the interpolation is clearly excellent and in practical terms this gives us the opportunity of using equation (12), with consequent savings in computer time, in the determination of the temperature dependence of the relaxation rate described in the next section. The deviation of $\bar{\tau}$ from the Arrhenius rule is obvious for all spin concentrations other than 0.5. This concentration seems to hold the balance between the two extreme jump rate distributions, which cause opposite deviations from $e^{-\hat{\mathcal{E}}/\Theta}$. The MC results seem to imply that the effect is simply a consequence of the way in which the thermodynamics of filling the energy wells changes with concentration. At low concentration the sites act as traps for the diffusing spin which become relatively deeper at lower temperatures. Since there is a tendency for the deeper traps to be filled, $\bar{\nu}$ drops below $\hat{\nu}$. On the other hand, at high concentration most sites are occupied and trapping is less important since the vacancies tend to follow the paths marked out by the shallower traps for which ν diminishes

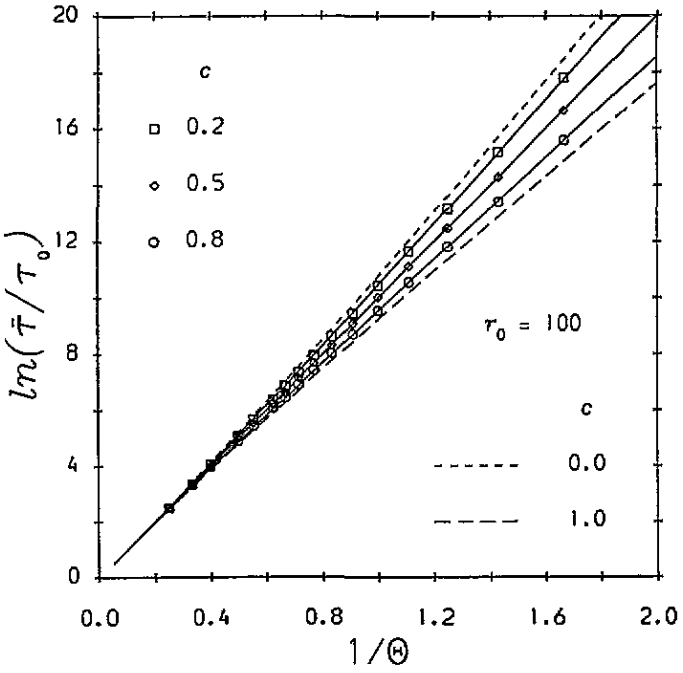

Figure 3. The data points obtained from the MC simulation demonstrate how the the mean interval between jumps, $\bar{\tau}$, deviates from the Arrhenius law when there is a spread of site energies. The solid lines through the data points are obtained from the interpolation given in equation (12) and show that the interpolation can be used to find the temperature dependence of the jump interval to high accuracy. The dashed lines, which are the extremes of the deviation at concentrations, $c = 0$ and 1, are calculated from equations (10) and (7), respectively.

less rapidly than $\hat{\nu}$ as the temperature falls.

These results have their counterparts in theoretical and MC calculations of Limoge and Bocquet (9) for the random walk of a single atom on a lattice with site and saddle energy disorder. The low-concentration results given above are consistent with the reduced diffusivity of the single atom found by Limoge and Bocquet when only site disorder is present, that is when trapping is predominant. On the other hand the trapping effect is absent for saddle disorder and the atom then tends to proceed along the path of least barrier height with very similar consequences for the mobility to that found in the high-concentration case. Limoge and Bocquet have pointed out that diffusion in experiments on disordered systems is usually found to have Arrhenius-like behaviour and have argued that this is the result of balance between the effects of the site and saddle disorder, both of which are likely to be present in real materials. Since it is reasonable to suppose that the effect of saddle disorder is, at least qualitatively, independent of composition, the present results show that in experiments with finite hydrogen concentration this balance can only be achieved at low concentration.

The departure from the Arrhenius form is only significant over a fairly large number of orders of magnitude in $\bar{\nu}$. Experiments, for example nuclear magnetic relaxation, are typically restricted to about three orders and it can be shown that the departure from Arrhenius behaviour is probably not large enough to be detected over this range. However, the MC simulation shows that the effective activation energy over this limited range, which could be measured experimentally, changes significantly with composition. This feature

could be used to detect the presence of disorder. It should be pointed out that this applies only to experiments which measure $\bar{\nu}$ directly since the root mean square distance travelled in the diffusion is reduced by correlation effects at high concentration [7].

5. The correlation functions and the relaxation rate

The longitudinal relaxation rate, T_1^{-1}, due to the random fluctuations in the magnetic coupling of the nuclear spin dipoles on the hydrogen atoms caused by the diffusion is [10]

$$T_1^{-1} = \tfrac{3}{2}\gamma^4\hbar^2 I(I+1)[J_1(\omega) + J_2(2\omega)]. \tag{14}$$

Here T_1 is the relaxation time, ω the Larmor frequency and J_1 and J_2 are the spectral densities of the time-dependent spin correlation functions $G_1(t)$ and $G_2(t)$. For present purposes $G_1(t)$ and $G_2(t)$ for a system with N_s spins are defined as [7]

$$G_m(t) = (1/N_s)\sum_{jk} F_{mjk}(0)F^*_{mjk}(t) \tag{15}$$

with

$$\begin{aligned} F_{1jk}(t) &= r_{jk}^{-3}\sin\theta_{jk}\cos\theta_{jk}\exp(-i\phi_{jk}) \\ F_{2jk}(t) &= r_{jk}^{-3}\sin^2\theta_{jk}\exp(-2i\phi_{jk}) \end{aligned} \tag{16}$$

where $m = 1$ or 2, the indices j and k run from 1 to N_s, $k \neq j$ and $r_{jk}\theta_{jk}\phi_{jk}$ are the co-ordinates of the vector between the spins j and k.

In order to calculate the time dependence of the spin correlation functions, MC runs were made in the manner described in the section on diffusion. The correlation functions were evaluated at each MC step after thermal equilibrium had been reached and in order to reduce the statistical errors many runs, each with the same $\rho(\nu)$ but with a different spatial disorder, were carried out. The final results were the mean values of the correlation functions taken of these runs and the nuclear magnetic relaxation rate was found from them by Fourier transform.

Typical results are shown in figures 4, 5 and 6 in which the normalized correlation functions for three different temperatures and spin concentrations, c, are plotted. Since $G_1(t)$ and $G_2(t)$ have no significant differences apart from the normalization factor the values of only one function at each temperature are plotted. The solid lines in the figure are the least-squares fits of the correlation functions to the sum of decaying exponentials. Five exponentials were used in the sum in order to give good fits for all times, t, used in the simulation. The unit of time has been chosen to be the mean time between diffusion hops, $\bar{\tau}$, calculated in the manner described in the previous section. Consequently, if there is no distribution of jump rates, all the normalized correlation functions for a given c would appear identical irrespective of temperature. When there is a distribution, lowering the temperature increases the spread and causes a change in shape of the correlation function which has the effect of reducing its overall rate of decay. The effect becomes less severe as c decreases.

The use of a sum of decaying exponentials for $G_m(t)$ allows their Fourier transforms, the spectral density functions, to be found analytically. Typically about 30 runs were used to find average values of $G_m(t)$ to which the sum of exponentials was fitted. This method also has the advantage of smoothing out statistical variations in $G_m(t)$ which can occur over periods of the order of τ. In the direct Fourier transformation of $G_m(t)$ these variations cause the spectral density function to fluctuate in turn about its mean value at large $\omega\tau$

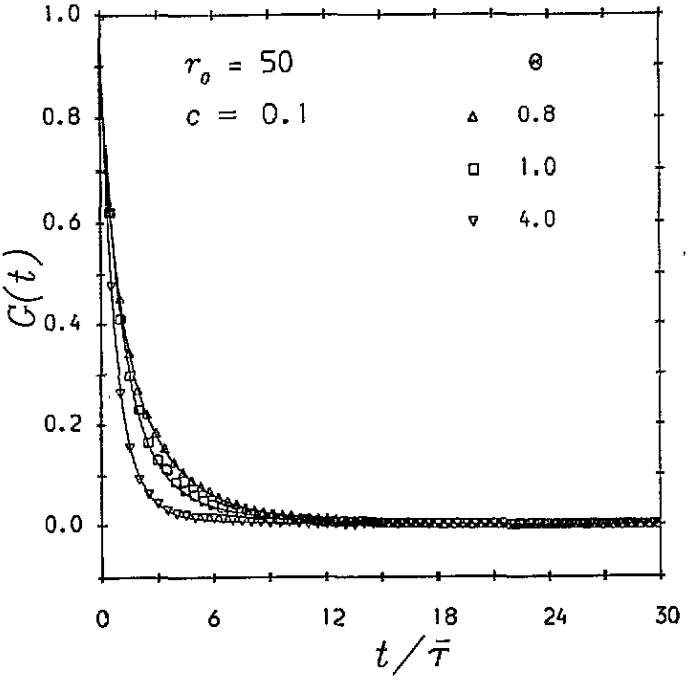

Figure 4. The normalized time-dependent spin correlation functions, $G(t)$, at various reduced temperatures, Θ. Here $G(t)$ stands for either $G_1(t)$ or $G_2(t)$ since after normalization they were found to be indistinguishable. The concentration of the spins is $c = 0.1$ and the parameter, r_0, which determines the spread of site energies, is 50. The data points are obtained from the MC simulation and the solid lines are obtained from the sum of five exponential functions as indicated in the text.

(~10). In order to keep these fluctuations to about 50% of the mean, typically 320 runs to calculate the average $G_m(t)$ are required. There is essentially no difference between this mean and the Fourier transform obtained from the exponential sum after 30 runs. The use of exponentials thus results in a considerable saving in computing time. Even if the fitting method is used it is still important to use a fairly large number of runs, especially in the first 5τ or so in the simulation of $G_m(t)$ because during this period the correlation functions change most rapidly and the quality of the data there affects the precision with which the spectral densities at large $\omega\tau$ can be determined.

The relaxation rates calculated from the correlation functions in figures 4–6 are shown by the solid lines in figures 7–9 in the form of logarithmic plots of ωT_1^{-1} against $\omega\bar{\tau}$. Since the principal aim of the simulation is to demonstrate the effect of disorder rather than give absolute values, the relaxation rates displayed in the figures are given in arbitrary computer units. They have been normalized by the spin concentration so that the maximal values are approximately the same for all the calculations. The previous figures 4–6 show that the distribution of jump rates causes an overall reduction in the decay rate of the spin correlation functions. Consequently the peak in the relaxation rate flattens and shifts towards smaller $\omega\tau$ as the temperature is lowered and spread in jump rates increases.

So far, $\rho(\nu)$ and $\bar{\nu}$ have been specified by the parameters r_0 and Θ, mainly to facilitate the discussion of the diffusion. It was shown in equations (4*a*) and (4*b*) that $\rho(\nu)$ can be equally well be expressed in terms r and the factor $\hat{\nu}$. It is easily shown from equation (8) that $f(\Theta, r_0)$ can be expressed in the same way. Consequently, in figures 4–6 the different

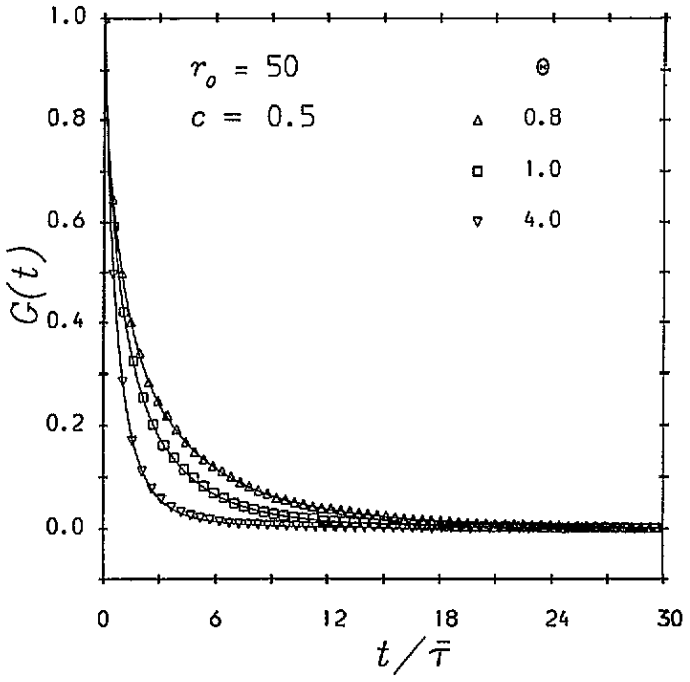

Figure 5. The normalized time-dependent spin correlation functions, $G(t)$, at various reduced temperatures, Θ, and concentration, $c = 0.5$. The meaning of the symbols is the same as in figure 4. The overall reduction in the decay rate of the correlation which results from the increase in the width of the distribution of jump rates when the temperature is lowered is clearly demonstrated.

correlation functions may be characterized by the parameter r rather than Θ and in fact the curves corresponding to $\Theta = 4$, 1 and 0.8 also correspond to $r = 2.7$, 50 and 133, respectively. The temperature appears in $\bar{\nu}$ but this simply scales the units of time which are given by $\bar{\tau}$. In the Fourier transforms of figures 7–9 the scaling occurs in ω which has units of $1/\bar{\tau}$. Thus the correlation functions and the corresponding relaxation curves may be regarded as having a fixed temperature and a characteristic distribution width, r. It should be noted that the units of frequency are not the same from curve to curve unless $f(\Theta, r_0)^{1-2c}$ happens to be equal to unity.

With these features in mind it is possible to make comparison with the calculations of Adnani *et al* [7]. The parameters adopted in the present simulation are not identical; nevertheless, inspection of the results shows that the shifts and increases in the widths of the peaks due to the disorder are comparable with those of the earlier work. For example, the curves with $r = 2.7$ reproduce approximately the peaks found in ordered systems and demonstrate that the maxima have the characteristic shift towards lower $\omega\tau$ as the spin concentration increases. The reader is referred to the earlier paper [7] for a discussion of the relaxation curves and a comparison with previous work in general. There is, however, one significant exception. In Adnani *et al* the peaks in ωT_1^{-1} were found to be almost symmetrical, whereas in the present work the slope of ωT_1^{-1} is generally greater on the low $\omega\tau$ side of the maximum. This asymmetry does not appear to arise from the improvement in the statistical accuracy of the present work but is due to systematic differences in the shape of the spin correlation functions. The cause may be the very different MC methods used in the two simulations. In the earlier simulation only one spin jumped at each MC

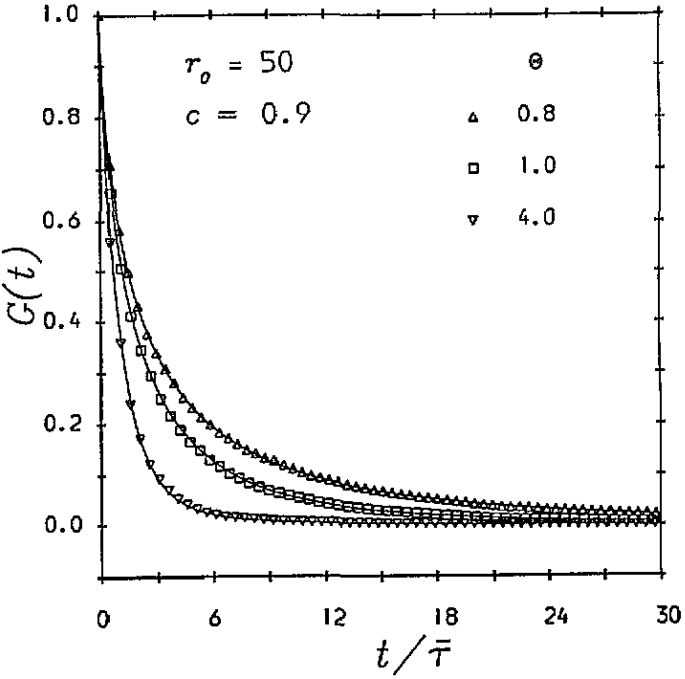

Figure 6. The normalized time-dependent spin correlation functions, $G(t)$, at various reduced temperatures, Θ, and concentration, $c = 0.9$. The meaning of the symbols is the same as in figure 4. Figures 4–6 show how the effect of the distribution in jump rates increases with spin concentration.

step, the choice of spin being determined by the various probability factors. In the present work a varying number of spins, around one tenth of the total, are allowed to make jumps. The two methods apparently lead to different decay rates of the correlation functions for times $t < \bar{\tau}$ even though there is general agreement overall.

The parameter ωT_1^{-1} has been chosen to emphasize that in figures 7–9 ω is the variable and $\bar{\tau}$ is a constant dependent on temperature. The Fourier transform of an exponentially decaying spin correlation function, $e^{-t/\tau}$, is $\tau/(1+\omega^2\tau^2)$ and, especially in regard to experiments, ω is usually held constant and τ is a variable dependent on temperature, giving rise to the characteristic maximum observed in T_1^{-1}. The extra factor ω is required to provide symmetry between these two parameters and give the peaks in the figures. It is possible to interpret the experimentally observed dependence of relaxation rate on temperature in ordered systems by means of such ωT_1^{-1} against $\omega\tau$ curves. The same can not be done for the disordered case unless it is possible to make allowance for the temperature dependence of $\rho(\nu)$ and $f(\Theta, r_0)$. In order to calculate a relaxation curve which accounts for these dependences in the present model it is necessary to choose a particular distribution of jump rates through the parameter r_0 and at each temperature carry out an MC simulation to find the correlation function and its spectral density. The output of the MC simulation is a family of curves of T_1 against $\ln(\omega\bar{\tau})$ with different values of Θ. The requisite values of T_1 follow the locus of a curve through this family giving T_1 as a function of $\omega\tau$ while simultaneously allowing $\omega\bar{\tau}$ and Θ to satisfy equation (12) and fixing ω at an appropriate value. The relaxation rate may then be obtained as a function of either $\omega\bar{\tau}$ or Θ.

In figures 10(a)–(c) the calculated values of the relaxation time, T_1, are plotted as a function of the reduced temperature for $c = 0.1, 0.5$ and 0.9 and the parameters $r_0 = 50$,

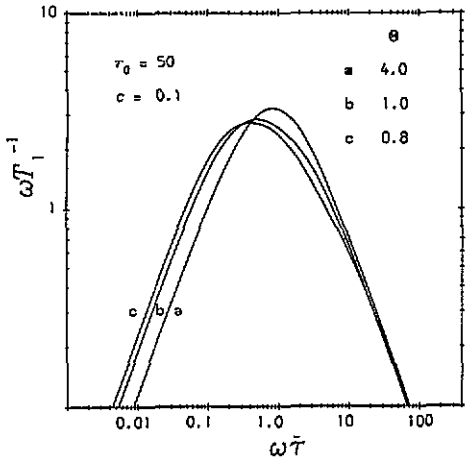

Figure 7. The relaxation rate, T_1^{-1}, obtained from the Fourier transform of the spin correlation functions given in figure 4. For comparison with earlier calculations of the relaxation rate, the figure plots the product ωT_1^{-1} in arbitrary computer units as a function of $\omega\bar{\tau}$, where ω is the nuclear Larmor frequency and $\bar{\tau}$ is the mean interval between jumps of the spins. As explained in the text, the distribution of jump rates for curve (a) is small and this curve is similar to the results of earlier calculations of the relaxation rate for ordered systems. The general shift to lower $\omega\bar{\tau}$ and the increase in width of the curves for lower temperatures at which the distribution is significant reflects the changes in the spin correlation functions.

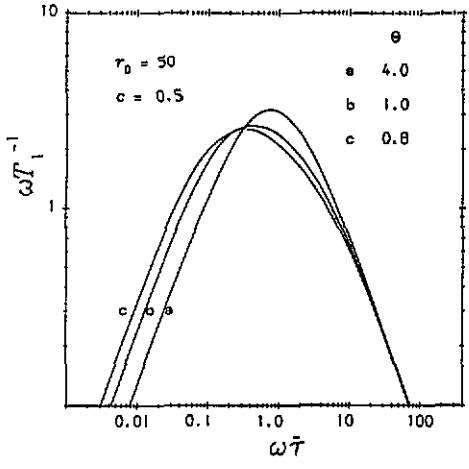

Figure 8. The relaxation rate, T_1^{-1}, obtained from the Fourier transform of the spin correlation functions given in figure 5. See the captions of figures 5 and 7 for the meaning of the curves and symbols.

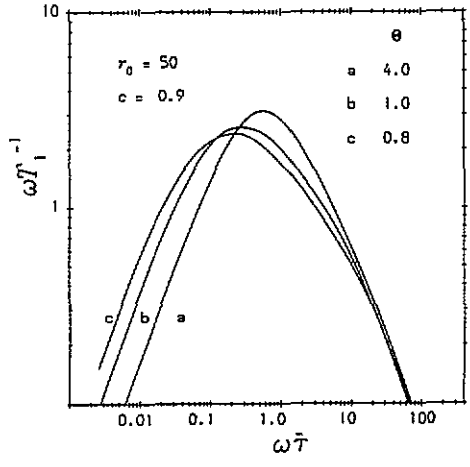

Figure 9. The relaxation rate, T_1^{-1}, obtained from the Fourier transform of the spin correlation functions given in figure 6. See the captions of figures 6 and 7 for the meaning of the curves and symbols.

$\hat{\mathcal{E}} = 10$ and $\omega\tau_0 = 1.7\times10^4$. The solid lines in these figures give T_1 for ordered systems, that is $r = 1$, and the relaxation time rather than the rate has been plotted since this parameter is normally used in experiments. Figure 10(b), for which $c = 0.5$, may be regarded as a plot of T_1 against either $1/\Theta$ or $\ln(\omega\bar{\tau})$ since these two variables are equivalent when $f(\Theta, r_0)^{1-2c}$

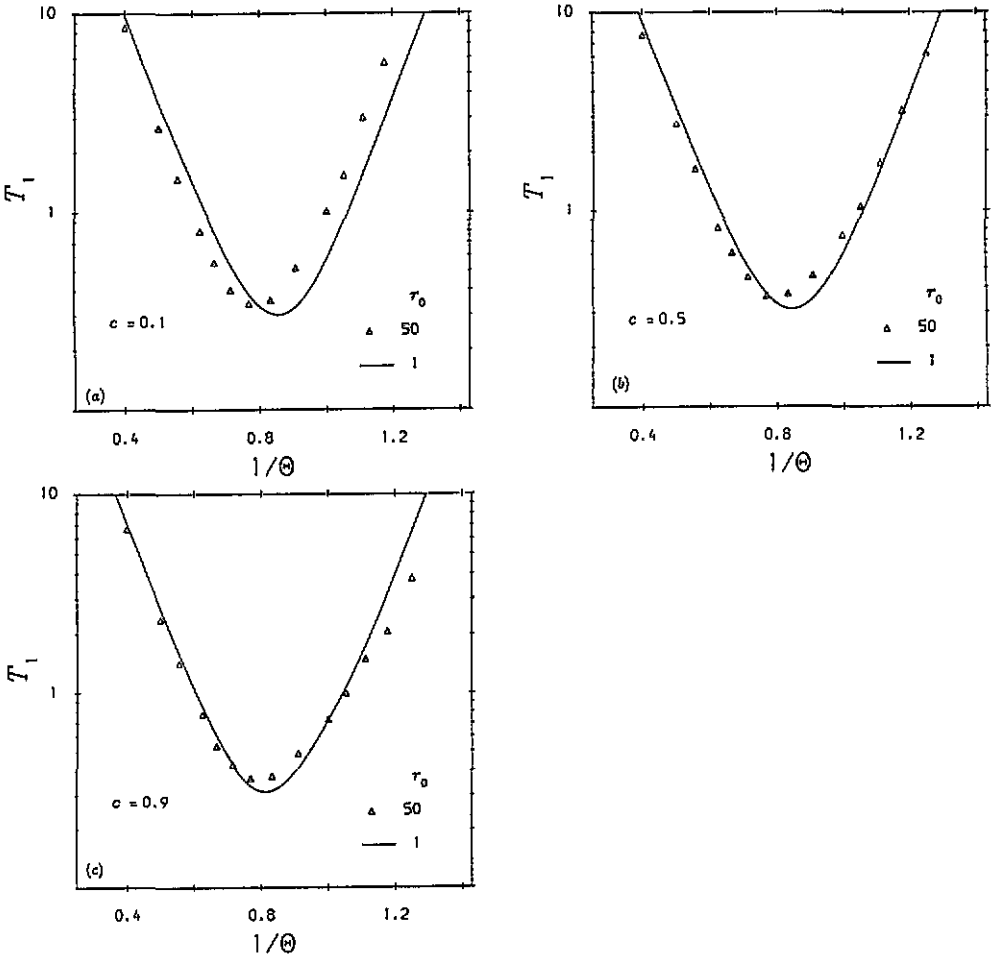

Figure 10. (a)–(c). The relaxation time, T_1, in arbitrary computer units obtained from the MC simulation as explained in the text and plotted as a function of the reciprocal temperature, $1/\Theta$, for spin concentrations, $c = 0.1$, 0.5 and 0.9 respectively. The solid line for $r_0 = 1$ is the relaxation time for an ordered system. When a distribution of jump rates ($r_0 = 50$) is present the dip in the relaxation time becomes asymmetrical having a smaller slope at low temperatures. The asymmetry increases with c. The shift of the minimum to higher temperatures is a consequence of the shifts in the relaxation curves in figures 7–9. This shift is apparently enhanced for $c = 0.1$ and reduced for $c = 0.9$ on account of the difference in the mean jump interval, $\bar{\tau}$, in the manner shown in figure 3. The dip in the relaxation also becomes broader as c increases, reflecting the difference in the temperature dependence (effective activation energy) of $\bar{\tau}$.

is equal to unity and $\bar{\tau}$ has the Arrhenius form. With this equivalence in mind it can be seen that the shift of the minimum in T_1 with respect to the solid line arises from the shifts of the relaxation curves towards lower $\omega\bar{\tau}$ in figure 8 as r_0 increases. The figure shows that once the temperature dependence of the jump rate distribution is taken into account the principal difference between the ordered and disordered cases lies in the asymmetry of the dip in the relaxation time.

In figures 10(a) ($c = 0.1$) and 10(c) ($c = 0.9$) the value of $\bar{\tau}$ is larger and smaller respectively than its value for $c = 0.5$ because of the opposite direction of the temperature dependence of $f(\Theta, r_0)^{1-2c}$ at high and low concentrations in the manner shown in figure 3.

Consequently, the shift of the minimum is slightly more pronounced in figure 10(a) and less in figure 10(b). The temperature dependence of $\bar{\tau}$ also changes so that the effective activation energy in figure 10(a) is greater than that in figure 10(c) and this is reflected in the difference in the width of the relaxation curves. It can also be seen that the asymmetry increases with c.

The main parameter which determines the form of the curves in figures 10(a)–(c) is r_0. If $T_0(\Theta = 1)$ is chosen to be 300 K, $\hat{E}$ then comes out to be ~0.25 eV and the minima occur in the region of 370–380 K. These values are commensurate with those derived from experimental relaxation rates of hydrogen in amorphous metals [5, 11, 12]. The value of $r_0 = 50$ is equivalent to $\delta E/\hat{E} = 0.4$, which is somewhat larger than the spread of activation energies found in internal friction measurements (13, 14). It would appear therefore that these parameters give the largest change with respect to the ordered case in the T_1 curves which is consistent with the experimental data. In fact, to increase r_0 to any significant extent would require a larger basic lattice in the simulation in order to be certain that there were a reasonable number of spins within a given $\delta\nu$.

These results show that, once its temperature dependence has been taken into account, the distribution of jump rates does not introduce any significant changes to the dip in the relaxation time apart from the asymmetry noted above. The changes in the width of the dip simply reflect differences in the effective activation energy. The asymmetry arises from three different causes, the temperature dependence of $f(\Theta, r_0)$, the asymmetry of the relaxation curves in figures 7–9 and the fact that drawing the locus through these curves in the manner indicated above results in a greater asymptotic slope at higher temperatures. The first cause may be disregarded since, as pointed out in the section on diffusion, the departure from the Arrhenius form over the temperature range of figure 10 is not significant. The third cause is also present in the calculations of Adnani *et al* [7] and the new results confirm the general characteristics of the relaxation rate found by the earlier work. The main difference is that the asymmetry is more pronounced in the present work because of the features indicated in the second cause given above. As pointed out in an earlier paragraph, these features arise in turn from the initial parts of the spin correlation functions, which are different in the two calculations.

The MC simulation has demonstrated that the best way of measuring the distribution of jump rates in a disordered metal–hydrogen system by means of nuclear magnetic relaxation is to measure the relaxation rate over a wide range of Larmor frequency at a given temperature. The method is technically demanding and probably requires the use of more than one spectrometer. It is unlikely that the simpler procedure of measuring T_1 as a function of temperature will set any value on the width of the distribution. However, the presence of the distribution may be detected through the asymmetry of the dip in T_1, which increases with spin concentration, and the change in the effective activation energy, which diminishes with concentration. These features of the nuclear magnetic relaxation, which have been clearly established in the present work, could not have been predicted in earlier calculations.

References

[1] Gillan M J 1991 *J. Less-Common Met.* **172/4** 529
[2] Torrey H C 1954 *Phys. Rev.* **92** 962
[3] Sholl C A 1981 *J. Phys. C: Solid State Phys.* **14** 447–64, 1479
[4] Sholl C A 1994 *Proc. Int. Symp. on Metal–Hydrogen Systems (Fuji-Yoshida, 1994)*
[5] Crouch M A, Havill R L and Titman J M 1986 *J. Phys. F: Met. Phys.* **16** 99
[6] Richards P M and Shinar J 1987 *J. Phys. F: Met. Phys.* **17** 1659

[7] Adnani N, Havill R L and Titman J M 1994 *J. Phys.: Condens. Matter* **6** 2999
[8] McDowell A F and Cotts R M 1994 *Z. Phys. Chem.* **183** 65
[9] Limoge Y and Bocquet J L 1990 *Phys. Rev. Lett.* **65** 60
[10] Abragam A 1961 *The Principles of Nuclear Magnetism* (Oxford: Clarendon)
[11] Bowman R C Jr, Maeland A J and Rhim W-K 1982 *Phys. Rev.* B **26** 6362
See also
Bowman R C Jr *et al* 1984 *J. Non-Cryst. Solids* **61/2** 649
[12] Dolde K, Messer R and Stoltz U 1984 *Proc. 5th Int. Conf. on Rapidly Quenched Metals (Würzberg, 1984)*
[13] Berry B S and Pritchet W C 1981 *Phys. Rev.* B **24** 2299
[14] Hazelton L E and Johnson W L 1984 *J. Non-Cryst. Solids* **61/2** 667